ACS OMEGA

http://pubs.acs.org/journal/acsodf

Article

Unsaturated Polyester Resin as a Nonformaldehyde Adhesive Used in Bamboo Particle Boards

Zhenzeng Wu,* John Tosin Aladejana, Shuqiong Liu, Xinhuai Gong, Xiaodong Alice Wang, and Yongqun Xie*

Cite This: *ACS Omega* 2022, 7, 3483−3490

Read Online

ACCESS | Metrics & More | Article Recommendations | Supporting Information

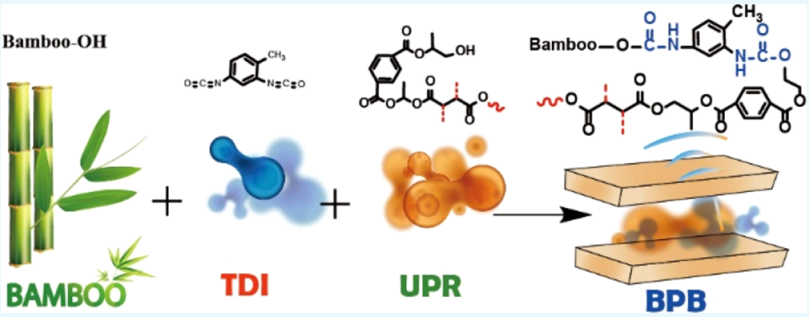

ABSTRACT: Unsaturated polyester resin (UPR) with good chemical resistance, excellent mechanical properties, and formaldehyde-free shows great potentials in the wood industry. In this study, the mechanical strength, thermostability, dynamic thermomechanical property, and interfacial bonding of bamboo particle boards (BPBs) made from UPR adhesives with toluene diisocyanate (TDI) as the coupling agent were explored. The results showed that covalent bonds were formed among TDI, bamboo particles, and UPR, which could significantly enhance the mechanical strength. The internal bonding strength, modulus of elasticity, and modulus of rupture of treated BPBs were 1.36, 3010, and 19.6 MPa with the increment of 1250, 514, and 833%, respectively, compared to the control samples. Also, the thickness swelling rate of the BPB was 4.6%, much lower than that of the control, with a decrease of 92%. The thermostability of the treated BPB was also improved. As a result, the BPB using UPR as the adhesive and TDI as the coupling agent shows better usability, higher efficiency, and excellent mechanical strength.

1. INTRODUCTION

Bamboo, commonly known as "the second forest", is abundant in Southwest China.[1,2] As a sustainable, readily available, and biodegradable material with a short maturity rotation (4−5 years), bamboo is widely employed as a notable nontimber building material for flooring and furniture manufacturing (e.g., bamboo particle board (BPB), bamboo mat board, laminated bamboo board, bamboo scrimber, and bamboo mat veneer composite).[3−6] One of the key challenges in a bamboo-based board is the release of a carcinogenic substance from formaldehyde-based adhesives widely used in the wood industry.[7−9] Nonformaldehyde-based adhesives, such as cornstarch,[10] soy protein,[11,12] magnesium oxychloride,[13] and aluminophosphate,[14] have attracted extensive attention owing to them being formaldehyde-free, nontoxic, having rich sources, and so forth. However, the use of such adhesives is also limited by the poor fungal resistance, complicated fabrication process, and weak wet bonding strength.[15]

Unsaturated polyester resin (UPR) is formed through a typical polycondensation process and addition reaction. Maleic anhydride, saturated dicarboxylic acid, and several polyhydric alcohols were used in the first step, and vinyl monomers were introduced in the second stage.[16,17] UPR has the advantages of low density, design flexibility, good acidity and alkali resistance, outstanding mechanical performance, and cost-effectiveness, which could be used in automobiles, aircraft, and electric appliances as a substitute for traditional materials.[18−22] However, all the previous investigations focus on the composite of UPR as the matrix and different fibers as reinforced materials.[23,24] UPR could be one of the most promising nonformaldehyde adhesives used in the wood industry.[25] The resultant polyester adhesive could be cured at a lower temperature and shorter time using suitable initiators and accelerators. Due to the big polarity gap between bamboo fibers and UPR, their interface bonding force could be very weak. The phenol-formaldehyde resin was introduced as an interface-modifying agent to solve this problem since UPR

Received: October 25, 2021
Accepted: January 5, 2022
Published: January 18, 2022

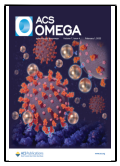

https://doi.org/10.1021/acsomega.1c05969
ACS Omega 2022, 7, 3483−3490

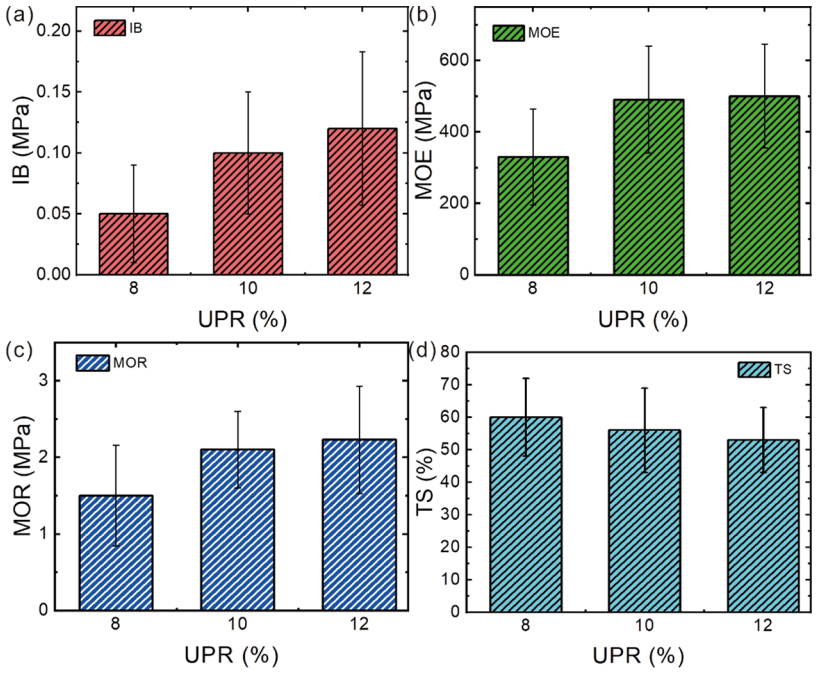

Figure 1. mechanical performance of BPBs showing the addition of UPR with different (a) IB, (b) MOE, (c) MOR, and (d) TS.

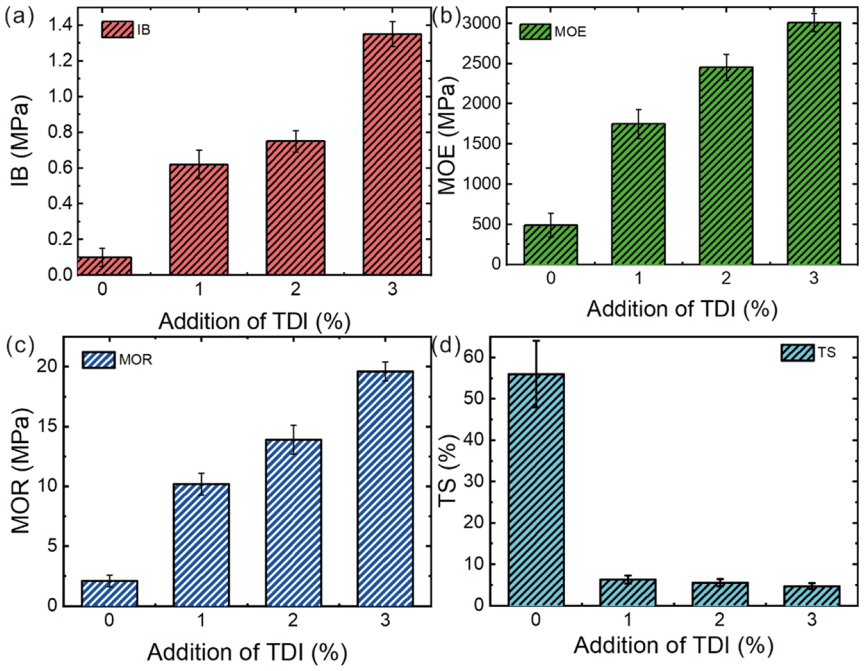

Figure 2. mechanical performance of BPBs showing the addition of TDI with different (a) IB, (b) MOE, (c) MOR, and (d) TS.

is amphipathic.[26] Unfortunately, the interface-modifying agent of phenol formaldehyde is harmful to humans.

Isocyanates with a highly active functional group of −NCO could react with compounds containing active hydrogen atoms (amine, alcohol, water, etc.), widely used as coupling agents for the surface treatment of glass, carbon, and natural fibers.[27−29] Toluene diisocyanate (TDI), methylenediphenyl diisocyanate, hexamethylene diisocyanate, and isophorone diisocyanate are common isocyanates used in industries. With double −NCO groups, TDI could be used as a coupling agent and cross-link with different compounds or molecular chains. TDI was used in the paper coating field, where the mechanical strength of the treated paper was apparently enhanced, and a bridge structure was formed between wood fibers, especially at the cross-point of the fibers.[30]

The readily available bamboo processing residue could be recycled and utilized as a raw material in this study. The UPR as a formaldehyde-based adhesive and TDI as a coupling agent for fabricating the BPB have not been reported. The preparation, mechanical strength, thermostability, and interfacial adhesion mechanism between the adhesive and bamboo are investigated by using a mechanical testing machine, thermogravimetric (TG) analysis, dynamic thermomechanical

https://doi.org/10.1021/acsomega.1c05969
ACS Omega 2022, 7, 3483−3490

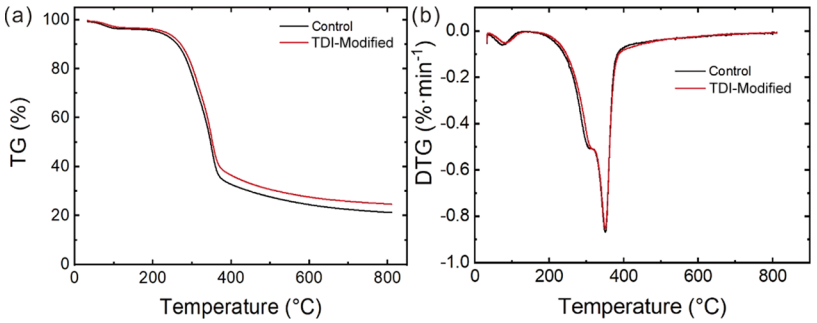

Figure 3. Thermostability property of BPBs: (a) TG curves and (b) derivative TG curves.

analysis (DMA) test, Fourier transform infrared (FTIR) spectroscopy, and X-ray photoelectron spectroscopy (XPS).

2. RESULTS AND DISCUSSION

2.1. Mechanical Properties of BPBs. The mechanical properties of BPBs with the addition of various UPRs are shown in Figure 1. All these three levels of UPR showed similar mechanical properties, which were much lower than the values of the standard level. The reason could be that there is a big polarity gap and no covalent bond connection between the bamboo fiber and UPR, resulting in their poor interfacial bonding force. Apparently, there were two steps of change of mechanical properties with the increase of the UPR from 8 to 12%. Moreover, in the first step from 8 to 10% of the UPR, the mechanical properties' increment was much more distinct than that in the second step. In this case, the addition of 10% of UPR was chosen to prepare the BPB.

The influence of different adhesives such as UF + MDF, citric acid/starch, silicon magnesium, magnesium oxychloride, and soy-based adhesives on the property of the internal bonding strength (IB) used in BPBs is compared in Figure S1 in the Supporting Information. The control samples (i.e., without TDI) showed poor interface adhesion performance with 0.1 MPa IB (Figure 2a). However, as the TDI addition increased, the IB improved steadily. The IBs of the samples with the addition of TDI of 1, 2, and 3% were higher than those of the control ones by 6.2, 7.5, and 13.5 times, respectively. Similarly, the modulus of elasticity and rupture (MOE and MOR, respectively) test samples presented in Figure 2b,c follow the same increasing trends. When TDI was added at 1, 2, and 3%, the MOE increased by 257.1, 400, and 514.3%, respectively, compared to the control samples. Also, the MOR increased by 385.7, 561.9, and 833.3%, with the addition of TDI of 1, 2, and 3%, respectively. In Figure 2d, the thickness swelling (TS) of the TDI-modified samples was much lower than that of the control samples (56%). The TSs at 1, 2, and 3% of TDI were lower by 6.3, 5.5, and 4.7%, respectively. Therefore, the higher mechanical strength and the lower TS of the fabricated BPB indicate better interface bonding performance.

2.2. Thermostability Property of the BPBs. The thermostability properties of the control and TDI-modified samples (3% of TDI) are shown in Figure 3 and Table 1. The total weight loss (WL) of the control samples is 78.8% (Figure 3a). It can be seen in the figure that there are three stages of WL [i.e., at 35−115 °C (3.1% of WL), 115−380 °C (62.4% of WL), and 380−800 °C (13.3% of WL)]. The three WL stages could be due to the evaporation of physically absorbed water, pyrolysis stage with the highest WL, and carbonization stage,

Table 1. TG Key Parameter Comparison of the BPB Samples[a]

BPB samples	temperature of peak WL (°C)			temperature stages of WL (°C)		
	T_{p1}	T_{p2}	T_{p3}	T_{30}	T_{50}	T_{70}
control	73.88	310.45	350.63	314.60	347.34	446.97
TDI-modified	83.98	316.55	350.55	322.07	352.11	517.76

[a]Note: T_{p1}: temperature of the first peak WL; T_{p2} and T_{p3}: temperature of the second and third peaks WL. T_{30}: temperature of 30% WL; T_{50} and T_{70}: temperatures of 50 and 70% WL, respectively.

respectively.[8,31] Contrary to the control samples, the TDI-modified samples exhibited a lower total WL of 75.3%, indicating better fixation of the char residue's ability. Moreover, the temperatures of the first peak WL (T_{p1}) and T_{p2} are 10.1 and 6.1 °C higher than the control ones, respectively (Figure 3b and Table 1). The control and modified samples have almost the same T_{p3}. The temperature stages of T_{30}, T_{50}, and T_{70} are 7.47, 4.77, and 70.79 °C higher than those of the control ones, respectively. These results show that TDI improves the thermal stability of the BPBs. The reason for the improvement of the thermal stability may be that the TDI functions as a coupling agent and enhances the internal portions to form a more tightly coupled group.

2.3. Dynamic Thermomechanical Analysis of the BPBs. DMA tests could help to understand the dynamic thermomechanical behavior of composites. The storage modulus versus temperature and tan delta versus the temperature curves of control and TDI-modified samples (3% of TDI) are presented in Figure 4. As shown in Figure 4a, both curves undergo a sharp drop between 40 and 80 °C and then begin to decline gently. The storage modulus of the TDI-modified samples was higher than that of the control. The elastic state modulus of the modified samples overlaid the control ones. This may be attributed to the phase change of the UPR from the glassy to a rubbery state. Moreover, the UPR in the BPB functions as an adhesive and not as the usual composite's matrix. As observed, bamboo particles (BPs) create a cross-linked structure, which upholds the framework of the BPB. Consequently, the storage modulus of the modified samples altered slightly. Tan delta reveals the motion of the molecular chain in the composites. The temperature of the tan delta' peak in the TDI-modified samples shows 1.26 °C overlaying the peak of the control samples. Summarily, there may be a connection between the UPR molecular chain and the BPs in the treated BPB, while weak interfacial compatibility is observed in the untreated BPB. This confirms that TDI as a coupling agent enhances the interaction of the UPR and BPs.

https://doi.org/10.1021/acsomega.1c05969
ACS Omega 2022, 7, 3483−3490

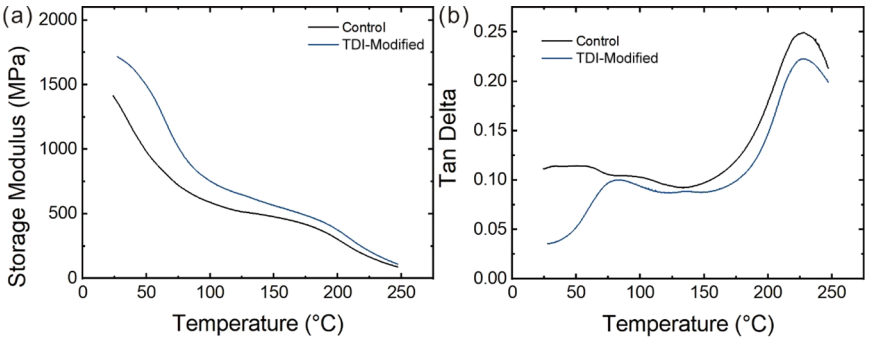

Figure 4. DMA curves of the control and TDI-modified samples: (a) storage modulus and (b) tan delta as a function of temperature.

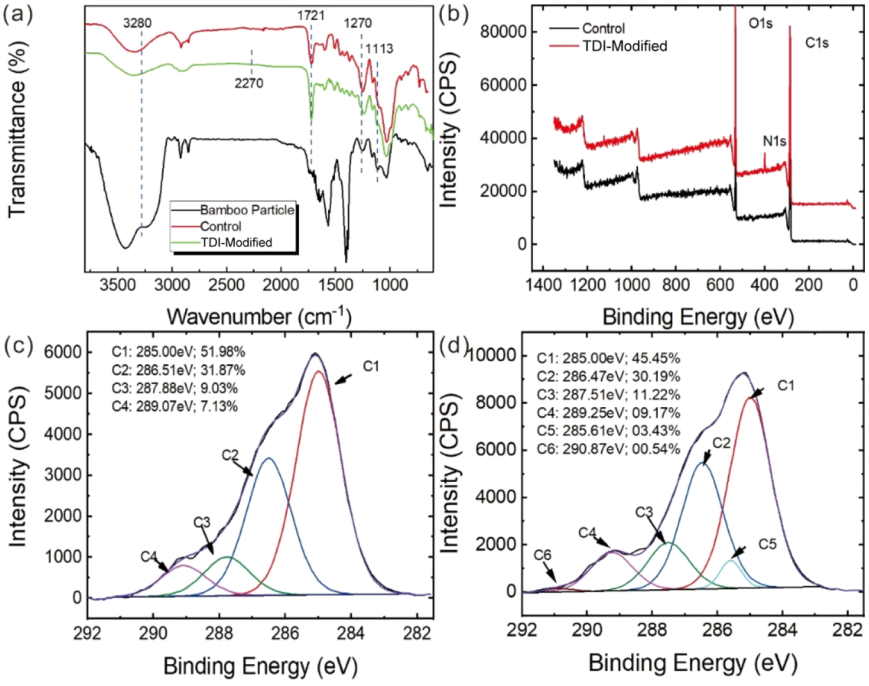

Figure 5. Surface chemical functional group and the BPB bond: (a) FTIR curve, (b) XPS survey spectra of the control and TDI-modified sample, (c) curve-resolved spectra of the XPS C 1s peak of control, and (d) TDI-modified sample.

2.4. Reaction Mechanism of Interface Adhesion. As shown in Figure 5a, the typical FTIR spectral characteristic peaks of the lignocellulosic material showed three main components: cellulose, hemicellulose, and lignin. These peaks are located at 3341, 2918, 2848, 1720, 1597, 1506, 1453, 1410, 1156, 895, 830, and 729 cm^{-1}, which could be attributed to the OH and H−bonding stretching, $-CH_3$ stretching, $-CH_2-$ methylene symmetry stretch vibration, C═O stretching, C═C stretching of the aromatic ring (lignin), C═C stretching of the aromatic ring (lignin), asymmetric bending of $-CH_3$, aromatic skeletal vibrations (lignin), in-plane C−H deformation (cellulose), C−O−C asymmetrical stretching of carbohydrates, b-glycosidic linkages, and C−H out-of-plane and C−CH_2 rock, respectively.[32] Compared to the BPs and control sample spectra, the peaks of the TDI-modified samples (3% of TDI) are located at 1113, 1721, and 3280 cm^{-1}, attributed to the O−C−O characteristic absorption of aliphatic ethers,[33] the C═O group of the urethane linkage (which results in the reaction of −NCO with −OH from the bamboo surface or UPR),[34,35] and the N−H stretching of urethane amide,[36] respectively. Usually, the peak around 2270 cm^{-1} is attributed to the terminal −NCO, but it is absent in the spectrum of the TDI-modified sample. Therefore, the coupling agent of TDI connected the bamboo fiber and UPR with a chemical bond of C−N, occurring in the absence of free −NCO groups.

In order to explore the mechanism of interface bonding, an XPS test was performed, and the result is shown in Figure 5b−d and Table 2. The percentage of N element and N/C of the treated samples is higher, and the O/C percentage values are lower than those in the control samples due to the addition of TDI (i.e., low O/C ratio and high N/C ratio). This indicates that TDI was successfully fixed in the BPB (Table 2).[37]

Table 2. Contents of Oxygen, Carbon, and Nitrogen Elements, with Their O/C and N/C Ratios of Different Samples, Were Determined by XPS

	element concentration (%)			atomic percentage	
samples	C	O	N	O/C	N/C
control	68.63	29.96	1.41	44	2
TDI-modified	66.41	28.18	5.42	42	8
TDI (theoretical)	62.07	20.69	16.09	33	26

https://doi.org/10.1021/acsomega.1c05969
ACS Omega 2022, 7, 3483−3490

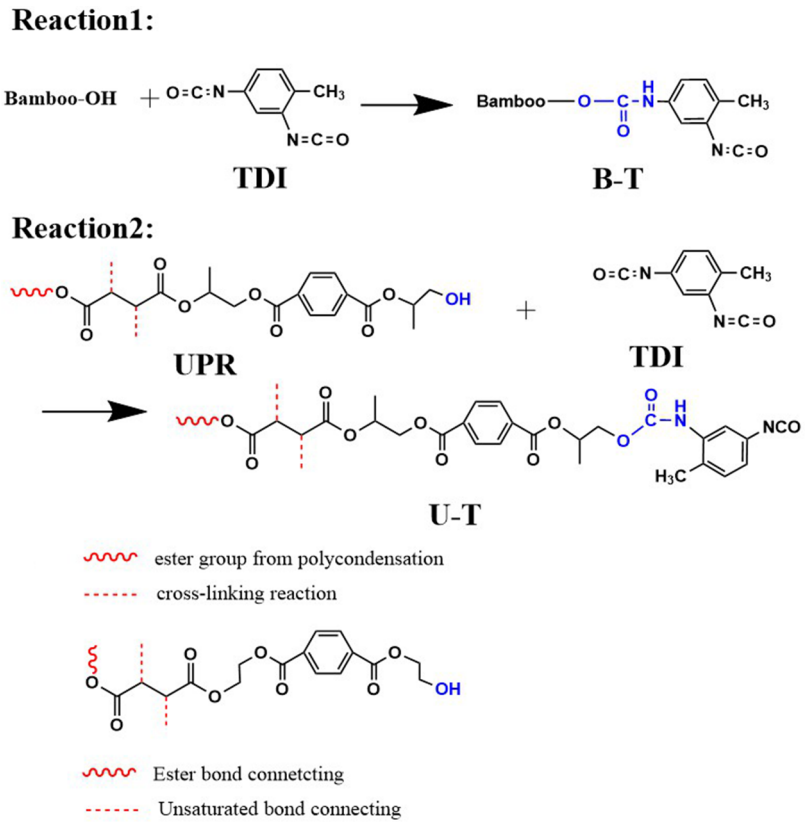

Figure 6. Proposed reactions in the TDI-modified UPR BPB.

As shown in Figure 5b, the N element reflected in the TDI-modified sample (3% of TDI) indicates that TDI reacted with UPR and BPs. The percentage of C2 (C−OH groups) values decreased dramatically from 31.87% of the control samples to 30.19% of the modified samples (Figure 5c,d). Contrarily, the percentage of C3 (C═O groups) and C4 (O−C═O groups) of the modified samples increased by 2.19 and 2.04%, respectively, compared to the control samples. This increment may be due to the TDI reaction with the C−OH groups during UPR and BP connection, thereby reducing C1 while C3 and C4 increased. Moreover, the spectra of TDI-treated samples further revealed two new peaks: C5 (C−N groups) and C6 (−N═C═O groups). Their percentage was 3.97%, accounting for the carbamate reactant from −NCO of TDI and −OH of the bamboo particle or UPR.

The BPB interfacial reactions could be established based on the analyses presented, as shown in Figure 6. In reaction 1, the hydroxy groups of bamboo surface could react with the isocyanate of TDI to form the B-T unit, and in reaction 2, the hydroxy of UPR could react with the isocyanate of TDI to form the U-T unit. Based on these two basic reactions, the real connection among bamboo, UPR, and TDI could be B-T-B, B-T-U, and U-T-U units because of the double isocyanates of TDI, which built more complex three-dimensional network structures in the BPBs. The covalent bond was built between the BPs and UPR, resulting in tight interfacial connections and reduction in moisture absorption (i.e., lower TS). The mechanism promotes significant improvement of mechanical strength and thermostability of the BPBs.

3. CONCLUSIONS

UPR as a nonformaldehyde adhesive was chosen to produce BPBs. TDI as a coupling agent connecting UPR and the BPs was investigated in BPBs. A covalent bond connects TDI, BPs, and UPR, significantly enhancing the mechanical strength and reducing moisture absorption (i.e., 92% decrease in TS). Compared to the control samples, the IB, MOE, and MOR of the modified samples were 1.36, 3010, and 19.6 MPa with an increment of 1250, 514, and 833%, respectively. The thermostability of the BPBs was improved. As a result, UPR as a nonformaldehyde adhesive could be used in BPBs because it shows better usability, higher efficiency, and excellent mechanical strength.

4. MATERIALS AND METHODS

4.1. Materials. BPs (Zhejiang Dasso Group Co., Ltd., Hangzhou, China) were used to prepare BPBs. UPR (YY-330 of o-type and the structure shown in Figure 1, 6.2 mg of KOH/g acid value, 320 mPas viscosity at 25 °C, 64.2% solid content, and 494 s gelling time), cobalt naphthenate, and methyl ethyl ketone peroxide (1 wt % Co element) were supplied by Yongyue Science & Technology Co., Ltd. (Quanzhou, China). TDI was bought from Shanghai Aladdin Biochemical Technology Co., Ltd. (Shanghai, China). The chemical structures of UPR and TDI are shown in Figure 7.

https://doi.org/10.1021/acsomega.1c05969
ACS Omega 2022, 7, 3483−3490

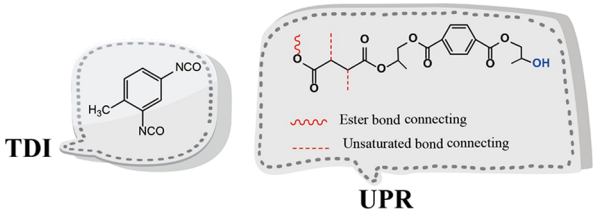

Figure 7. Chemical structures of UPR and TDI.

4.2. Methods. *4.2.1. Preparation of the BPBs.* The UPR (10 wt % of dry BP) was first mixed with cobalt naphthenate (accelerator, 1.0 wt % of UPR) and methyl ethyl ketone peroxide (initiator, 1.0 wt % of UPR), which severs as the adhesive to fabricate BPBs (preparation process shown in Figure 8). The TDI (0−3% of UPR) was added dropwise into

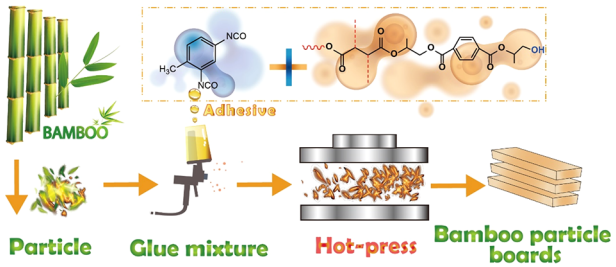

Figure 8. Preparation process of the BPBs.

UPR with even stirring. The BPs (8% of moisture content) were sprayed with the prepared UPR (with and without TDI) in a laboratory particle blender (25KG, Hebei Forest Machinery Factory, China). After mixing with the adhesive, the BP was placed in a rectangle mold (350 mm × 350 mm × 10 mm). Subsequently, the molded BP was transferred to a hot-press machine (BY302X2/15, Suzhou Xinxieli Machine Manufacturing Co., Ltd., Suzhou, China) to form the BPBs (control and TDI-modified samples). The hot-pressing temperature, pressure, and time were 160 °C, 1.0 MPa, and 5 min, respectively.

4.2.2. Materials Characterization. The mechanical strength of the BPB was tested by using a mechanical testing machine (MTS, USA). A constant load rate of 10 mm/min was applied according to the standard of GB/T 9846−2015.[38] The sample size for evaluating the IB and TS was 50 mm × 50 mm × 10 mm ($L \times W \times H$). The MOE and MOR test sample size was 200 mm × 50 mm × 10 mm. The reported results were the average of 10 samples. DMA was performed using DMA Q800 V20.22 Build 41 (TA instruments New Castle, DE, USA). The samples were cut in the dimensions of 35 mm × 10 mm × 4 mm ($L \times W \times H$). The test mode, temperature range, and heating rate were single cantilever bending mode, 30−250 °C, and 5 °C/min, respectively. The frequency and amplitude were 1 Hz and 20 μm, respectively. The functional groups of the BPBs were tested by a Nicolet 380 FTIR (Thermal Electron Instruments, USA) system with the KBr disk method. The testing scans, resolutions, and range were 64, 4 cm^{-1}, and 4000−400 cm^{-1}, respectively. The chemical bond connection of the interface of the BPBs between bamboo and UPR was spotted by XPS (ESCALAB 250, USA). The test was carried out in an ultrahigh-vacuum system with Al Kα radiation at room temperature. The pass energy, spot size, and energy step were 100 eV, 500 μm, and 1.00 eV, respectively. The thermostability property of the BPB was tested by using thermogravimetric (TG, NETZSCH STA 449F3, Germany) analysis. The thermostability property was analyzed under a nitrogen atmosphere at a heating rate of 10 °C min^{-1} and in the temperature range of 20−800 °C.

4.2.3. Statistical Analysis. One-way analysis of variance (ANOVA) was conducted with the data from the tests using the Excel 2016 software program (Microsoft Co. Ltd., USA). The results from ANOVA showed significant differences at the confidence level of 95%..

■ ASSOCIATED CONTENT

Supporting Information

The Supporting Information is available free of charge at https://pubs.acs.org/doi/10.1021/acsomega.1c05969.

Comparison of the IB property of different adhesives used in BPBs (PDF)

■ AUTHOR INFORMATION

Corresponding Authors

Zhenzeng Wu − *The College of Ecology and Resource Engineering, Wuyi University, Wuyishan City, Fujian 354300, P.R. China;* orcid.org/0000-0002-9046-9667; Email: zhenzeng.wu@wuyiu.edu.cn

Yongqun Xie − *The College of Material Engineering, Fujian Agriculture and Forestry University, Fuzhou, Fujian 350002, P.R. China;* orcid.org/0000-0001-8466-5680; Phone: +86 591 83789307; Email: fjxieyq@hotmail.com

Authors

John Tosin Aladejana − *The College of Material Engineering, Fujian Agriculture and Forestry University, Fuzhou, Fujian 350002, P.R. China*

Shuqiong Liu − *The College of Ecology and Resource Engineering, Wuyi University, Wuyishan City, Fujian 354300, P.R. China*

Xinhuai Gong − *The College of Ecology and Resource Engineering, Wuyi University, Wuyishan City, Fujian 354300, P.R. China*

Xiaodong Alice Wang − *The Department of Wood and Forest Sciences, Laval University, Quebec G1V 0A6, Canada*

Complete contact information is available at: https://pubs.acs.org/10.1021/acsomega.1c05969

Notes

The authors declare no competing financial interest.

■ ACKNOWLEDGMENTS

This work was financed by the Scientific Research Foundation of Wuyi University (YJ201913, 2020-SSTD-09), Fujian Educational and Scientific Research Projects for Young and Middle-Aged Teachers (JAT190785), and Fujian Natural Science Foundation (Youth Innovation) (2020J05219).

■ ABBREVIATIONS AND NOTATION LIST

UPR, unsaturated polyester resin; TDI, toluene diisocyanate; BP, bamboo particle; BPB, bamboo particle board; IB, internal bonding strength; TS, thickness swelling; MOE and MOR, modulus of elasticity and modulus of rupture, respectively; DMA, dynamic thermomechanical analysis test; XPS, X-ray photoelectron spectroscopy; TG, thermogravimetry; ANOVA, analysis of variance; WL, weight loss

https://doi.org/10.1021/acsomega.1c05969
ACS Omega 2022, 7, 3483−3490

REFERENCES

(1) Li, J.; Xu, H.; Yu, Y.; Chen, H.; Yi, W.; Wang, H. Intelligent analysis technology of bamboo structure. Part I: The variability of vascular bundles and fiber sheath area. *Ind. Crops Prod.* **2021**, *174*, 114163.

(2) Qi, J.; Xie, J.; Yu, W.; Chen, S. Effects of characteristic inhomogeneity of bamboo culm nodes on mechanical properties of bamboo fiber reinforced composite. *J. Foraminiferal Res.* **2015**, *26*, 1057−1060.

(3) Hao, J.; Yi, X.; Zong, G.; Song, Y.; Wang, W.; Cheng, H.; Wang, G. Fabrication of long bamboo fiber-reinforced thermoplastic composite by extrusion and improvement of its properties. *Ind. Crops Prod.* **2021**, *173*, 114120.

(4) Zhang, Y. M.; Yu, Y. L.; Yu, W. J. Effect of thermal treatment on the physical and mechanical properties of phyllostachys pubescen bamboo. *Eur. J. Wood Prod.* **2013**, *71*, 61−67.

(5) Mahdavi, M.; Clouston, P. L.; Arwade, S. R. A low-technology approach toward fabrication of laminated bamboo lumber. *Constr. Build. Mater.* **2012**, *29*, 257−262.

(6) Sulastiningsih, I. M.; Nurwati. Physical and mechanical properties of laminated bamboo board. *J. Trop. For. Sci.* **2009**, *21*, 246−251.

(7) Wu, Z.; Huang, D.; Wei, W.; Wang, W.; Wang, X.; Wei, Q.; Niu, M.; Lin, M.; Rao, J.; Xie, Y. Mesoporous aluminosilicate improves mildew resistance of bamboo scrimber with Cu B P anti-mildew agents. *J. Clean. Prod.* **2019**, *209*, 273−282.

(8) Wu, Z.; Chen, T.; Aladejana, J. T.; Kouomo Guelifack, Y.; Li, D.; Hou, X.; Wang, X.; Niu, M.; Xie, Y. Hierarchical lamellar aluminophosphate inorganic materials for medium density fiberboard with good fire performance. *J. Ind. Eng. Chem.* **2021**, *98*, 180−188.

(9) Chen, T.; Wu, Z.; Liu, Z.; Aladejana, J. T.; Wang, X.; Niu, M.; Wei, Q.; Xie, Y. Hierarchical porous aluminophosphate-treated wood for high-efficiency solar steam generation. *ACS Appl. Mater. Interfaces* **2020**, *12*, 19511−19518.

(10) Oktay, S.; Kızılcan, N.; Bengu, B. Oxidized cornstarch - Urea wood adhesive for interior particleboard production. *Int. J. Adhes. Adhes.* **2021**, *110*, 102947.

(11) Chen, S.; Chen, H.; Yang, S.; Fan, D. Developing an antifungal and high-strength soy protein-based adhesive modified by lignin-based polymer. *Ind. Crops Prod.* **2021**, *170*, 113795.

(12) Sun, Z.; Sun, B.; Bai, Y.; Gao, Z. Economical improvement on the performances of a soybean flour-based adhesive for wood composites via montmorillonite hybridization. *Composites, Part B* **2021**, *217*, 108920.

(13) Zhou, W.; Ye, Q.; Shi, S. Q.; Fang, Z.; Gao, Q.; Li, J. A strong magnesium oxychloride cement wood adhesive via organic-inorganic hybrid. *Constr. Build. Mater.* **2021**, *297*, 123776.

(14) Chen, T.; Wu, Z.; Wang, X. A.; Wang, W.; Huang, D.; Wei, Q.; Wu, B.; Xie, Y. Hierarchical lamellar aluminophosphate materials with porosity as ecofriendly inorganic adhesive for wood-based boards. *ACS Sustain. Chem. Eng.* **2018**, *6*, 6273−6280.

(15) Ferreira, E. G. A.; Marumo, J. T.; Franco, M. K. K. D.; Yokaichiya, F.; Vicente, R. 10000 years cement - Can hydrated cement last as much as long-lived radionuclides? *Cement Concr. Compos.* **2019**, *103*, 339−352.

(16) Chu, F.; Qiu, S.; Zhang, S.; Xu, Z.; Zhou, Y.; Luo, X.; Jiang, X.; Song, L.; Hu, W.; Hu, Y. Exploration on structural rules of highly efficient flame retardant unsaturated polyester resins. *J. Colloid Interface Sci.* **2022**, *608*, 142−157.

(17) Yeo, J.-S.; Lee, J.-H.; Hwang, S.-H. Effects of lignin on the volume shrinkage and mechanical properties of a styrene/unsaturated polyester/lignin ternary composite system. *Composites, Part B* **2017**, *130*, 167−173.

(18) Zhang, N.; Hou, X.; Cui, X.; Chai, L.; Li, H.; Zhang, H.; Wang, Y.; Deng, T. Amphiphilic catalyst for decomposition of unsaturated polyester resins to valuable chemicals with 100% atom utilization efficiency. *J. Clean. Prod.* **2021**, *296*, 126492.

(19) Huang, B.-Z.; Zhao, L.-J. Bridging and toughening of short fibers in SMC and parametric optimum. *Composites, Part B* **2012**, *43*, 3146−3152.

(20) Kandelbauer, A.; Tondi, G.; Zaske, O. C.; Goodman, S. H. Unsaturated Polyesters and Vinyl Esters. In *Handbook of Thermoset Plastics*, 3rd ed.; William Andrew Publishing: Boston, 2014; pp 111−172.

(21) Zhang, Z.; Zhang, H.; Liu, T.; Lv, W. Study on the micro-mechanism and structure of unsaturated polyester resin modified concrete for bridge deck pavement. *Constr. Build. Mater.* **2021**, *289*, 123174.

(22) Bing, N.; Yang, J.; Gao, H.; Xie, H.; Yu, W. Unsaturated polyester resin supported form-stable phase change materials with enhanced thermal conductivity for solar energy storage and conversion. *Renew. Energy* **2021**, *173*, 926−933.

(23) Rahman, M. T.; Asadul Hoque, M.; Rahman, G. T.; Gafur, M. A.; Khan, R. A.; Hossain, M. K. Study on the mechanical, electrical and optical properties of metal-oxide nanoparticles dispersed unsaturated polyester resin nanocomposites. *Results Phys.* **2019**, *13*, 102264.

(24) Chu, F.; Yu, X.; Hou, Y.; Mu, X.; Song, L.; Hu, W. A facile strategy to simultaneously improve the mechanical and fire safety properties of ramie fabric-reinforced unsaturated polyester resin composites. *Composites, Part A* **2018**, *115*, 264−273.

(25) Singh, M.; Kadian, S.; Manik, G. Polymers in Adhesive Applications. In *Reference Module in Materials Science and Materials Engineering*; Elsevier, 2021.

(26) Li, R.; Lan, C.; Wu, Z.; Huang, T.; Chen, X.; Liao, Y.; Ye, L.; Lin, X.; Yang, Y.; Zheng, Y.; Xie, Y.; Zhuang, Q. A novel particleboard using unsaturated polyester resin as a formaldehyde-free adhesive. *Constr. Build. Mater.* **2017**, *148*, 781−788.

(27) Sathish, S.; Karthi, N.; Prabhu, L.; Gokulkumar, S.; Balaji, D.; Vigneshkumar, N.; Ajeem Farhan, T. S.; AkilKumar, A.; Dinesh, V. P. A review of natural fiber composites: Extraction methods, chemical treatments and applications. *Mater. Today: Proc.* **2021**, *45*, 8017−8023.

(28) Lin, Q.; Wu, J.; Yu, Y.; Huang, Y.; Yu, W. Immobilization of ferric tannate on wood fibers to functionalize wood fibers/diphenylmethane di-isocyanate composites. *Ind. Crops Prod.* **2020**, *154*, 112753.

(29) Attard, T. L. Toughened carbon-fiber reinforced epoxy via isophorone diisocyanate amine surface modification. *Polymer* **2020**, *191*, 122268.

(30) Tu, Q.; Meng, X.; Sun, M. The application of blocked waterborne polyurethane in paper coating. *Pap. Chem.* **2012**, *24*, 18−21.

(31) Wang, H.; Jia, N.; Xin, Y. Thermogravimetric analysis experiment and kinetic analysis of wood. *Fire Sci. Technol.* **2017**, *36*, 1209−1212.

(32) Jiao, Y.; Wan, C.; Li, J. Synthesis of carbon fiber aerogel from natural bamboo fiber and its application as a green high-efficiency and recyclable adsorbent. *Mater. Des.* **2016**, *107*, 26−32.

(33) Chen, S.; Wang, Q.; Wang, T. Preparation, tensile, damping and thermal properties of polyurethanes based on various structural polymer polyols: effects of composition and isocyanate index. *J. Polym. Res.* **2012**, *19*, 9994.

(34) Chen, S.; Wang, Q.; Wang, T. Damping, thermal, and mechanical properties of polycaprolactone-based PU/EP graft IPNs: effects of composition and isocyanate index. *J. Macromol. Sci., Part B: Phys.* **2012**, *51*, 83−95.

(35) Merlin, D. L.; Sivasankar, B. Synthesis and characterization of semi-interpenetrating polymer networks using biocompatible polyurethane and acrylamide monomer. *Eur. Polym. J.* **2009**, *45*, 165−170.

(36) Clemitson, I. R. *Castable Polyurethane Elastomers*, 2nd ed.; CRC Press: New York, 2015.

(37) Liu, W.; Chen, T.; Qiu, R. Effect of fiber modification with 3-isopropenyl-dimethylbenzyl isocyanate (TMI) on the mechanical properties and water absorption of hemp-unsaturated polyester (UPE) composites. *Holzforschung* **2014**, *68*, 265−271.

https://doi.org/10.1021/acsomega.1c05969
ACS Omega 2022, 7, 3483−3490

(38) *China National Standardization Management Committee, GB/T 9846-2015, in Plywood for General Use*; Standardization Administration of China: Beijing, China, 2015.

https://doi.org/10.1021/acsomega.1c05969
ACS Omega 2022, 7, 3483−3490